Methods

Case report

A 6-year-old previously healthy Japanese girl was admitted to our hospital because of positivity for proteinuria and microscopic hematuria that had been determined in a routine school medical examination. On admission, the patient was excessively alert, agitated, and anxious; her pulse rate was 150/min and blood pressure was 130/80 mmHg. A physical examination revealed a diffusely enlarged thyroid. Thyroid function tests revealed hyperthyroidism: the free-thyroxine level was 4.98 ng/dL (normal range 0.95–1.74 ng/dL; 64.1 pmol/L), free-triiodothyronine was 13.4 pg/mL (2.13–4.07 pg/mL; 20.6 pmol/L), and thyroid-stimulating hormone (TSH) was below 0.003 μU/mL (0.34–3.88 μU/mL; 0.003 mU/L). Serum anti-thyroglobulin was positive at a low titer (1:100×4, normal up to 100) , but anti-microsomal (= antithyroid peroxidase antibody, anti-TPO) antibody was moderately positive ($1:100\times4^2$, normal up to 100). The TSH-receptor antibody was positive at 84% (up to ±10%), and thyroid-stimulating antibody (TSAb) was 898% (up to 180%). We therefore diagnosed her as having Graves' disease and started medication with thiamazole. Her thyroid function rapidly normalized, but her microscopic hematuria (30–50 red blood cells per high-power field) and proteinuria [urinary protein to creatinine ratio, 4.32 g/g (489 g/mol)] continued. One month after the initial evaluation, she underwent a renal biopsy. Her clinical course is shown in Fig. 1. Her anti-nuclear antibody was negative, and serum circulating immune complexes were negative based on testing by multiple methods [fixed C1q-enzyme-linked immunosorbent assay (ELISA) and monoclonal rheumatoid factor (RF)-enzyme immunoassay (EIA)].

Light microscopy examination showed focal mesangial proliferation without thickening of the glomerular capillary walls or spike formation. However, granular IgG, C1q, and C3 deposition was detected along the glomerular capillary wall by a routine direct immunofluorescence method using fluorescein-isothiocyanate (FITC)-labeled antibodies against human IgG, IgA, IgM, C1q, C4, C3, and fibrinogen (Cappel, Aurora, OH). Electron microscopy examination revealed electron-dense deposits in the subepithelial spaces (Fig. 2). These findings are consistent with stage I MN.

Following renal biopsy, we treated the patient with the angiotensin-converting enzyme inhibitor (ACEI) lisinopril to reduce her proteinuria. Three months after the initiation of lisinopril therapy, her proteinuria was resolved.

Immunofluorescence study for TPO and thyroglobulin

The concomitant occurrence of thyroid and renal lesions in this case led us to suspect that thyroid-associated antigen-antibody complexes may have been responsible for the renal involvement. To investigate the relationship between the membranous nephropathy and Graves' disease, we stained frozen sections from a renal biopsy specimen for TPO and thyroglobulin using the immunofluorescence technique. Serial sections were incubated with monoclonal antibody against human TPO (TPO47; BioCytex, Marseille, France; not diluted) and with FITC-labeled monoclonal antibody against human thyroglobulin (B34.1; Abcam, Cambridge, UK; not diluted), washed, and then stained with FITC-labeled goat anti-mouse IgG (Cappel,

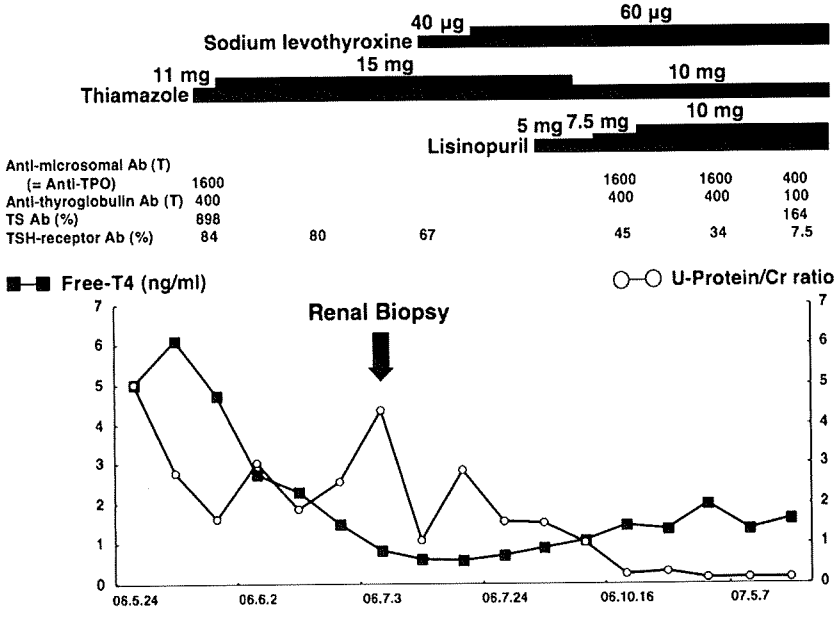

Fig. 1 Clinical course of the present patient suffering from membranous nephropathy associated with Graves' disease. *Ab* Antibody, *TPO* thyroid-peroxidase, *TS* thyroid-stimulating, *TSH* thyroid-stimulating hormone, *U* urinary, *Cr* creatinine, *T4* thyroxine

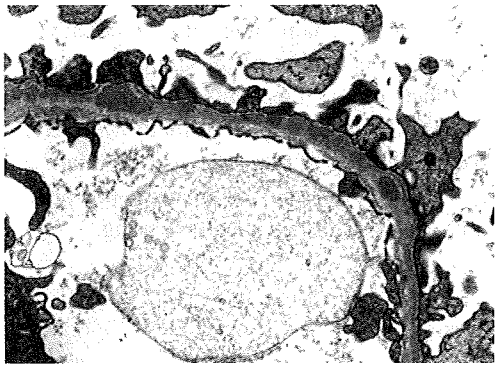

Fig. 2 Electron micrograph of a glomerulus from the patient. There are electron-dense deposits located in the subepithelial and intramembranous spaces. Original magnification 3000×

Aurora, OH; diluted to 1:10) for TPO. Sections from human thyroid gland were used as positive controls. The primary antibodies were omitted in the negative controls. Sections from a renal biopsy tissue showing minor glomerular abnormality were stained by the same procedure to serve as histological negative controls.

Results

The presence of TPO antigen was demonstrated as a granular pattern in glomeruli from the patient, corresponding to the granular deposits of IgG (Fig. 3a,b), while thyroglobulin was not detected (Fig. 3c). The secondary antibody alone produced a negative stain of TPO in the patient. There was no stain in sections from a renal biopsy tissue showing minor glomerular abnormality as the negative control using the same methods. Sections from human thyroid gland showed a positive stain for thyroglobulin using the same methods. We therefore concluded that the MN in this case had very likely been caused by immune complexes related to TPO.

Discussion

Renal involvement in thyroid diseases is a relatively rare event. However, two conditions have been recognized. One is anti-neutrophil cytoplasmic antibody (ANCA)-positive crescentic glomerulonephritis as a complication of treatment with propylthiouracil [4, 5]. The other is MN associated with autoimmune thyroid diseases, such as Hashimoto's and Graves' diseases, in which a considerable proportion of patients have thyroid-associated antigens, such as thyroglobulin and TPO [6–15]. In the latter condition, the development of MN may be associated with administration of ^{131}I [8, 14].

Since the presumed cause of MN is the deposition of immune complexes [1], the co-occurrence of Graves' disease and MN led us to suspect that immune complexes involving thyroid-associated antigen–antibodies were responsible for MN in this situation. The release of thyroid-associated antigens, such as thyroglobulin, from the thyroid may ultimately lead to MN [6–15]. It is believed that ^{131}I therapy may cause MN as a result of antigens released from the ablated thyroid tissue [8,14].

In 1969, Weigle and Nakamura first reported the production of autoimmune thyroiditis and nephritis in rabbits immunized with thyroglobulin [16]. In 1976, the first clinical case of MN related to autoimmune thyroiditis (Hashimoto's thyroiditis) was reported by O'Regan et al. [6]. To our knowledge, there have been only seven English-language reports of MN associated with Graves' disease (total 11 cases) [8–11, 13–15]. Immunofluorescence studies of thyroglobulin were carried out in five of the 11 cases [8, 9, 11, 13, 14], and deposits of thyroglobulin were proven in only four [8, 9, 11, 13].

In the present case, deposits of thyroglobulin were not proven, but the presence of deposits of TPO along the glomerular capillary walls was confirmed. Although there have been a few reports of MN associated with Hashimo-

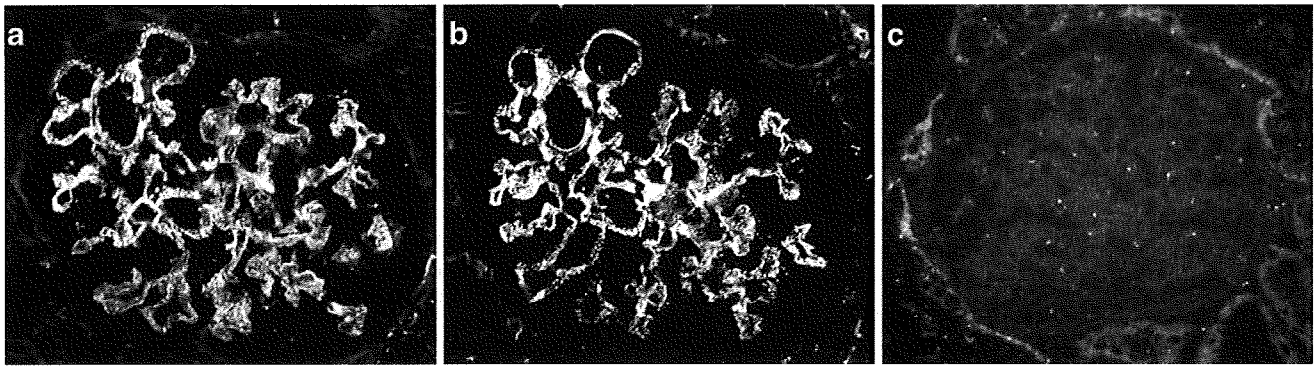

Fig. 3 Immunofluorescent glomerular staining for IgG (**a**), thyroid-peroxidase (**b**), and thyroglobulin (**c**). Serial sections were stained using fluorescein-isothiocyanate (FITC)-labeled antibodies against human IgG (**a**), monoclonal antibody against human thyroid-peroxidase (**b**), and FITC-labeled monoclonal antibody against human thyroglobulin (**c**). FITC-labeled goat anti-mouse IgG was used as a secondary antibody for thyroid-peroxidase. Original magnification 400×

to's disease showing positive staining for both thyroglobulin and TPO in the kidney [6, 7, 12], no previous studies of MN with Graves' disease have examined both thyroglobulin and TPO in the kidney. The case we present here is the first to have been reported in which both thyroglobulin and TPO were examined in the kidney, and it is also the first reported case of MN associated with autoimmune thyroid disease in which deposits of only TPO, and not thyroglobulin, were confirmed by immunohistochemistry. The positive immunofluorescent glomerular staining for TPO corresponding to granular deposits of IgG supports the contention that TPO antigen–antibody immune complexes were the cause of MN in this case. In our patient, serum anti-thyroglobulin was positive at a low titer (1:100 × 4, normal up to 100), but anti-microsomal (= anti-TPO) antibody was moderately positive ($1:100\times4^2$, normal up to 100). These titers are consistent with the findings from the immunofluorescence microscopy examination for TPO and thyroglobulin in the kidney. We performed the immunofluorescence stainings for IgG and TPO on the serial sections; however, a better approach may be to localize IgG and TPO on a section by confocal microscopy. However, stainings using complete serial sections are still a powerful tool.

With regard to the negative staining using anti-thyroglobulin antibody shown in Fig. 3c, we have to consider at least three different situations: (1) as we presume here, the observed result indicates the absence (or undetectable levels) of thyroglobulin in glomeruli; (2) the lack of staining simply represents a technical difficulty with this antibody (however, this is not likely since our use of human thyroid tissue as a positive control ensured that the antibody worked well under the staining conditions we used); (3) thyroglobulin is indeed present within glomerular immune deposits, but the epitope recognized by the antibody used here is masked or otherwise unavailable for binding. Thyroglobulin in deposits may be completely hidden by antibodies in immune complexes. Although the use of another antibody for thyroglobulin or an elution step to remove some of the bound antibodies may resolve this condition, unfortunately, the limitation in the amount of tissue available from the patient for testing did not allow us to confirm it. Therefore, the third condition remains unclear.

The molecular weights of thyroglobulin and TPO are approximately 660 and 100 kDa, respectively. The difference in molecular weights may influence the deposition and formation of the immune complex. In addition to size, charge and/or other physicochemical properties of TPO may facilitate its deposition in a subepithelial location.

We believe that treatment with thiamazole indirectly led to decreased circulating TSAb and TSH-receptor antibody, which in turn led to decreased stimulation of TPO synthesis/secretion and finally decreased the autoantibody (anti-TPO antibody = anti-microsomal antibody) level in our patient. Such a chain of events could have led to a reduction in the deposition of the immune complex in the kidney. In fact, during the clinical course of our patient, changes in TSAb/TSH-receptor antibody were concomitant with those of TPO (Fig. 1). The use of thiamazole may have been effective for the treatment of not only Graves' disease but also MN in this specific setting.

References

1. Makker SP (2004) Membranous nephropathy. In: Avner ED, Harmon WE, Niaudet P (eds) Pediatric Nephrology, 5th edn. Lippincott Williams & Wilkins, Philadelphia, pp 641–654
2. Cameron JS (1990) Membranous nephropathy in childhood and its treatment. Pediatr Nephrol 4:193–198
3. Takekoshi Y, Tanaka M, Shida N, Satake Y, Saheki Y, Matsumoto S (1978) Strong association between membranous nephropathy and hepatitis B surface antigenaemia in Japanese children. Lancet 2:1065–1068
4. Vogt BA, Kim Y, Jennette JC, Falk RJ, Burke BA, Sinaiko A (1994) Antineutrophil cytoplasmic autoantibody-positive crescentic glomerulonephritis as a complication of treatment with propylthiouracil in children. J Pediatr 124:986–988
5. D'Cruz D, Chesser AM, Lightowler C, Comer M, Hurst MJ, Baker LR, Raine AE (1995) Antineutrophil cytoplasmic antibody-positive crescentic glomerulonephritis associated with anti-thyroid drug treatment. Br J Rheumatol 34:1090–1091
6. O'Regan S, Fong JS, Kaplan BS, DeChadarevian JP, Lapointe N, Drummond KN (1976) Thyroid antigen-antibody nephritis. Clin Immunol Immunopathol 6:341–346
7. Jordan SC, Johnson WH, Bergstein JM (1978) Immune complex glomerulonephritis mediated by thyroid antigens. Arch Pathol Lab Med 102:530–533
8. Ploth DW, Fitz A, Schnetzler D, Seidenfeld J, Wilson CB (1978) Thyroglobulin–anti-thyroglobulin immune complex glomerulonephritis complicating radioiodine therapy. Clin Immunol Immunopathol 9:327–334
9. Horvath F Jr, Teague P, Gaffney EF, Mars DR, Fuller TJ (1979) Thyroid antigen associated immune complex glomerulonephritis in Graves' disease. Am J Med 67:901–904
10. Weetman AP, Pinching AJ, Pussel BA, Evans DJ, Sweny P, Rees AJ (1981) Membranous glomerulonephritis and autoimmune thyroid disease. Clin Nephrol 15:50–51
11. Jordan SC, Buckingham B, Sakai R, Olson D (1981) Studies of immune-complex glomerulonephritis mediated by human thyroglobulin. N Engl J Med 304:1212–1215
12. Iwaoka T, Umeda T, Nakayama M, Shimada T, Fujii Y, Miura F, Sato T (1982) A case of membranous nephropathy associated with thyroid antigens. Jpn J Med 21:29–34
13. Sato Y, Sasaki M, Kan R, Osaku A, Koyama S, Shibayama S, Sato M, Narumiya K, Takagi T, Kojima M (1989) Thyroid antigen-mediated glomerulonephritis in Graves' disease. Clin Nephrol 31:49–52
14. Becker BA, Fenves AZ, Breslau NA (1999) Membranous glomerulonephritis associated with Grave's disease. Am J Kidney Dis 33:369–373
15. Grcevska L, Polenakovic M, Petrusevska G (2000) Membranous nephropathy associated with thyroid disorders. Nephron 86:534–535
16. Weigle WO, Nakamura RK (1969) Perpetuation of autoimmune thyroiditis and production of secondry renal lesions following periodic injections of aqueous preparations of altered thyroglobulin. Clin Exp Immunol 4:645–657

Hum Genet
DOI 10.1007/s00439-009-0697-7

ORIGINAL INVESTIGATION

In vivo and in vitro splicing assay of *SLC12A1* in an antenatal salt-losing tubulopathy patient with an intronic mutation

Kandai Nozu · Kazumoto Iijima · Kazuo Kawai · Yoshimi Nozu · Atsushi Nishida · Yasuhiro Takeshima · Xue Jun Fu · Yuya Hashimura · Hiroshi Kaito · Koichi Nakanishi · Norishige Yoshikawa · Masafumi Matsuo

Received: 13 April 2009 / Accepted: 30 May 2009

Abstract Type I Bartter syndrome (BS), an inherited salt-losing tubulopathy, is caused by mutations of the *SLC12A1* gene. While several intronic nucleotide changes in this gene have been detected, transcriptional analysis had not been conducted because mRNA analysis is possible only when renal biopsy specimens can be obtained or occasionally when mRNA is expressed in the leukocytes. This report concerns a type I BS patient due to compound heterozygosity for the *SLC12A1* gene. Genomic DNA sequencing disclosed the presence of two novel heterozygous mutations of c.724 + 4A > G in intron 5 and c.2095delG in intron 16, but it remains to be determined whether the former would be likely to influence the transcription. In this report, we conducted both in vivo assay of RT-PCR analysis using RNA extracted from the proband's urinary sediments and in vitro functional splicing study by minigene construction, and obtained evidence that this intronic mutation leads to complete exon 5 skipping. To the best of our knowledge, this is the first study to use non-invasive methods for both an in vivo assay and an in vitro functional splicing assay of inherited kidney disease. These analytical assays could be adapted for all inherited kidney diseases.

K. Nozu (✉) · K. Iijima · Y. Nozu · A. Nishida · Y. Takeshima · X. J. Fu · Y. Hashimura · H. Kaito · M. Matsuo
Department of Pediatrics,
Kobe University Graduate School of Medicine,
Kusunokicho 7-5-1, Chuo, Kobe,
Hyogo 650-0017, Japan
e-mail: nozu@med.kobe-u.ac.jp

K. Kawai
Department of Pediatrics,
Matsusaka City Hospital, Mie, Japan

K. Nakanishi · N. Yoshikawa
Department of Pediatrics,
Wakayama Medical University,
Wakayama, Japan

Published online: 10 June 2009

Introduction

Inherited salt-losing tubulopathies with secondary hyperaldosteronisms, known as Bartter syndromes (BS) are autosomal recessive inherited disorders characterized by hypokalemic metabolic alkalosis accompanied by normal or low blood pressure despite hyperreninemia and hyperaldosteronemia. Recent genetic studies have found that these diseases are caused by mutations in one of the four genes, which lead, either directly or indirectly, to transporter or channel loss-of-function and are classified as type I-IV BS (OMIM 601678, 241200, 607364, and 602522, respectively) (Simon et al. 1996a, b; Simon et al. 1997; Birkenhager et al. 2001).

Patients with type I BS are characterized by impaired renal concentrating capacity and by hypercalciuria, resulting in the clinical characteristics of polyhydramnios and nephrocalcinosis. Type I BS usually arises during the antenatal to neonatal period, and is caused by mutations of the *SLC12A1* gene that encodes the Na–K–2Cl cotransporter (NKCC2) (Simon et al. 1996).

To date, more than 30 different mutations of the *SLC12A1* gene including intronic mutations outside the splice consensus sequence have been identified throughout the gene (Simon et al. 1996; Vargas-Poussou et al. 1998; Brochard et al. 2009). However, most of the studies to date have performed mutational analysis of the *SLC12A1* gene by using genomic DNA obtained from peripheral blood

leukocytes because kidney biopsy is rarely needed for these patients and the *SLC12A1* mRNA is not expressed in leukocytes. Although nucleotide changes in the intronic sequence have been reported, the exact nucleotide pathogenic mechanism has not been identified.

In the study reported here we performed an in vivo assay of RT-PCR analysis using mRNA extracted from urinary sediments and an in vitro functional splicing study using minigene construction in a Japanese female patient with type I BS. These splicing examination assays have the potential to be used for all inherited kidney diseases with intronic mutations.

Methods

Patient

The patient was a 7-year-old Japanese female with polyhydramnios who was the second of two siblings of healthy, non-consanguineous parents. Her elder sister also had polyhydramnios, was born prematurely and died with severe infection, but details including laboratory data were not available. The patient was born at 33 weeks' gestation complicated by polyhydramnios, and her birth weight was 1,830 g. She showed failure to thrive since 3 months after birth, milk vomiting was frequently seen with common cold and when she was 2 years old, she developed upper tract infection and showed severe dehydration, so she was referred to our hospital. At that time she showed hypokalemia (2.1 mEq/l) which continued after recovery. She was therefore suspected of having BS and a biochemical examination was conducted to establish a clinical diagnosis. At physical examination, her height was 85 cm (−2.1 SD). Her potassium level was low (2.1 mEq/l) and she had persistent metabolic alkalosis (pH 7.51). In spite of normal blood pressure, plasma renin activity (160 ng per ml per h; reference value: 0.5–2.0) and serum aldosterone (360 ng/dl; reference value: 56.9–150) levels were high, while serum magnesium (2.5 mg/dl; reference value: 1.7–2.5) level was normal. These findings led to a diagnosis of antenatal BS and treatment with potassium supply and spironolacton was started. At present she is 7 years old and 120.5 cm (−0.4SD) tall. She shows normal renal function (blood urea nitrogen: 6.7 mg/dl; Cr: 0.23 mg/dl) and high urine calcium excretion (urinary Ca/Cr: 0.63 mg/mg; reference value: 0.1–0.3). An abdominal sonographic study revealed bilateral medullary nephrocalcinosis.

Mutation analysis

After obtaining informed consent from the proband's parents, we performed genetic analysis of the *SLC12A1* gene in this family.

Isolation of DNA

DNA was isolated from peripheral blood samples in this family with standard phenol–chloroform extraction methods. Twenty-six primer pairs were generated to amplify all 26 exons including their exon-intron boundaries of the *SLC12A1* gene. Polymerase chain reaction (PCR) and the direct sequence method were used to determine the DNA sequence with an automated DNA sequencer (model 310; Applied Biosystems, Foster City, CA).

Extraction of total RNA

Total RNA was extracted from urine sediments, which were obtained by centrifugation at 1,500 rpm for 10 min from 100 mL of early morning urine. Microscopic examination of these sediments confirmed that there were sufficient renal tubular epithelial cells. RNA was isolated with the Isogen Kit (Nippon Gene Co., Toyama, Japan), and then reverse-transcribed into cDNA by using random hexamers and the Superscript III Kit (Invitrogen, Carlsbad, CA). cDNA was amplified by means of nested PCR with forward primers located in exon 3, and the reverse primer complementary to exon 7 (exon 3 first forward: CTGAAC ATCTGGGGAGTCATG; second forward: CTCCTGGAT TGTTGGAGAAGCTG; exon 7, first reverse: AGTTCCA ATGAAGAAGTTTGC; second reverse: GAAGAATGAC CAGAAGAATGAC). After 40 cycles of amplification, PCR products were separated on 2% agarose. In addition, PCR products were sequenced with a DNA sequencer (Perkin-Elmer-ABI, Foster City, CA). We used mRNA extracted from a healthy volunteer blood sample and urine to obtain normal control leukocyte and urinary sediments mRNA and the Human Kidney cDNA Library (Invitrogen) to obtain normal control kidney cDNA.

In vitro splicing assay

In our in vitro splicing experiments, hybrid minigene constructs were created by inserting a test sequence consisting of exon 5 and its flanking introns into the multicloning site within an intervening intron between two exons (exon A and B) of the minigene construct (H492) built in the pcDNA 3.0 mammalian expression vector (Invitrogen) (Fig. 1a) (Thi Tran et al. 2005; Tran et al. 2006). Each test sequence was obtained to amplify control sample and the proband's genomic DNA by PCR using primers that corresponded to introns 4 and 5, and included *Nhe*I and *Bam*HI restriction enzyme recognition sites, respectively (In5F-Nhe: 5′-CGCGCTAGC CCAAGAAGGGCTAAGTTATTCACTG-3′ and In5R-Bam: 5′-CGCGGATCCTGCGAGAACCTGGACTCAAA-3′). The amplified products were digested with *Nhe*I and *Bam*HI (New England Biochem, UK), and inserted into the

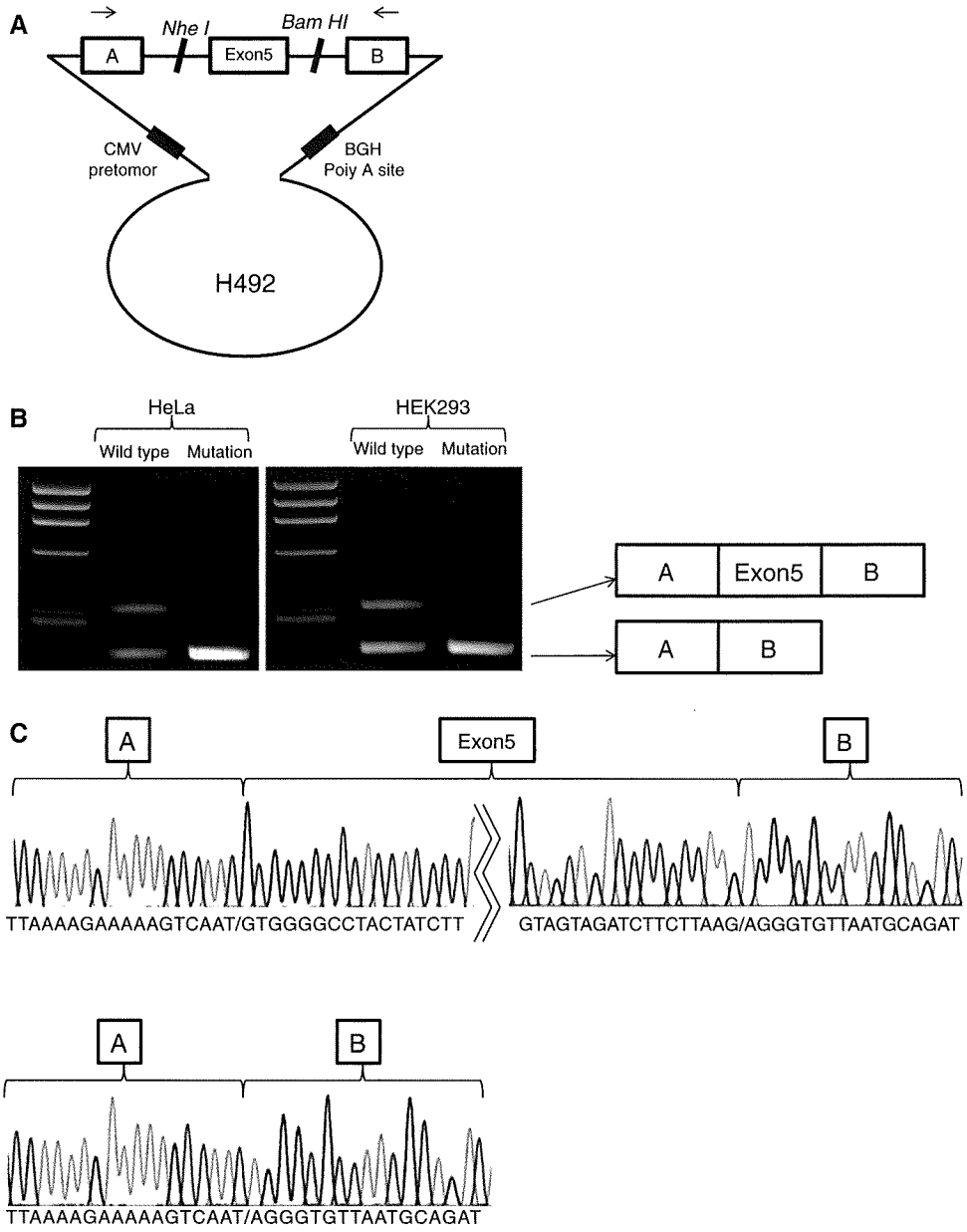

Fig. 1 Hybrid minigene tests in an in vitro splicing assay, **a** Schema of hybrid minigene construct A minigene (H492) was constructed to encode two cassette exons (A and B) and an intervening sequence containing a multicloning site. The minigene contained a cytomegalovirus (CMV) enhancer–promoter and a bovine growth hormone gene (BGH) polyadenylation signal (*black boxes*) for complete synthesis of mRNA. The primers used in the RT-PCR assay are represented by arrows. **b**, **c** RT-PCR amplified products of hybrid minigene transcripts. As shown in the gel file, a comparatively large band (329 bp) was present in the WT construct both in HeLa and HEK293 cells. In contrast, in the patient only a relatively small band (189 bp) was detected in both cell lines, which corresponds to skipping of exon 5 **b**. The PCR product containing the entire exon 5 sequence between cassette exons A and B was obtained from the minigene encoding the wild-type exon 5 since some of the product without exon 5 was present (**c** *top*). On the other hand, no product containing exon 5 could be obtained from the hybrid minigene containing exon 5 with the intronic mutation (**c** *bottom*)

minigene that had been digested with the same restriction enzymes. In this way, we constructed both wild-type and mutant hybrid minigenes that carried exon 5 with wild-type or mutated (c.724 + 4A > G) flanking introns, respectively. After their sequences had been confirmed, these hybrid minigenes were transfected into HeLa cells derived from cervical cancer cells and HEK293 cells derived from human embryonic kidney cells for splicing assays as described elsewhere (Thi Tran et al. 2005; Tran et al. 2006). Cells were harvested 24 h after the transfection and total RNA was extracted with the Isogen Kit. Five micrograms of total RNA was subjected to reverse transcription using random hexamer primers and the PCR was performed by using a forward primer corresponding to a segment of upstream exon A and a reverse primer complementary to a segment of the downstream exon B as previously described (Fig. 1) (Thi Tran et al. 2005). PCR products were analyzed by means of electrophoresis on an 8% polyacrylamide gel and with direct sequencing.

Results

Mutation analysis

Direct sequencing of the PCR-amplified products disclosed two novel mutations, one base substitution at the 4th base of intron 5 (c.724 + 4A > G) and one base deletion in exon

16 (c.2095delG) (Fig. 2). The same analyses of the parents' samples disclosed that the substitution was located on the maternal allele and the deletion on the paternal allele, which meant that the patient possessed the compound heterozygote of these two mutations. The substitution was not detected in 100 healthy control samples. It was therefore hypothesized that exon 5 from the maternal allele might have been skipped in the transcript. Exon 5 consists of 140 bp and when skipped in the transcript, will lead to the creation of premature stop codon in exon 6 (Fig. 3). The latter one base deletion mutation will also create premature stop codon in exon 16 immediately after the deletion mutation (Fig. 2).

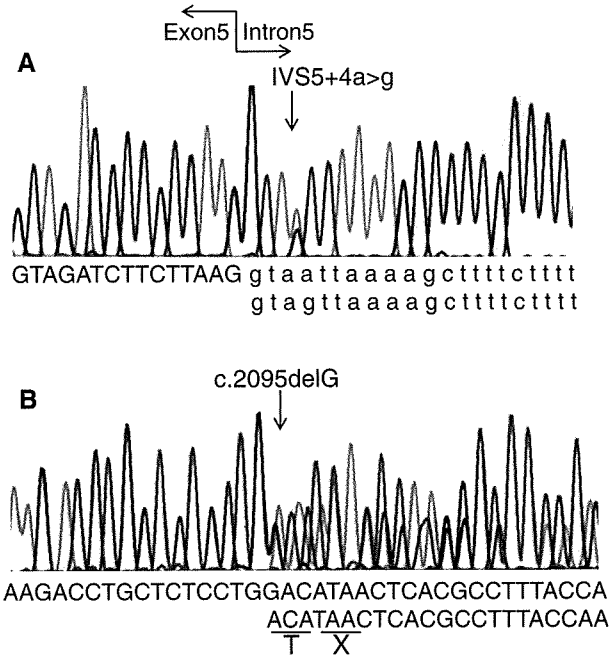

Fig. 2 Nucleotide changes in the SLC12A1 gene. **a** A heterozygous single-base substitution of A to G in intron 5 (c.724 + 4 A > G) was detected in the maternal allele. **b** A heterozygous 1-bp deletion at nucleotide 2095 located in exon 16 (c.2095 del G) was detected in the paternal allele

To confirm the inactivation of the splice-donor site, mRNA extracted from urinary sediments was used to amplify a fragment of exons 3–7 by means of reverse-transcription PCR (RT-PCR) with a pair of primers recognizing both exon 3 and 7. PCR products from the patient's sample showed two bands: one the same size as the control, and the other shorter (Fig. 3). Sequencing of the shorter product disclosed complete absence of the exon 5 sequences since exon 4 was directly joined to exon 6. This shorter band was not amplified in the normal kidney and urinary sediments. The RT-PCR results using mRNA extracted from leukocytes showed no bands, indicating that the leukocytes did not express mRNA of the *SLC12A1* gene.

In vitro splicing assay

Either the wild-type exon 5 or exon 5 with intronic mutation together with the flanking intron sequenceswas inserted into the preconstructed minigene to create hybrid minigenes, and their transcripts were analyzed by RT-PCR amplification. The PCR product containing the entire exon 5 sequence between the cassette exons A and B was obtained from the minigene encoding the wild-type exon 5 since a certain quantity of the product without exon 5 was present (Fig. 1b, c). On the other hand, the product containing exon 5 could not be obtained from the hybrid minigene containing exon 5 with the intronic mutation. A larger product corresponding to the product containing exon 5 and a smaller product without exon 5 were detected between exons A and B (Fig. 1b, c). The results indicated that the mutation-created disruption of the splicing donor site appeared in both the HeLa cells and HEK293 cells of this hybrid minigene. This confirmed that the c.724 + 4A > G mutation alone is responsible for the aberrant splicing.

Discussion

To date, about 30 different mutations of the *SLC12A1* gene have been identified throughout the gene in patients with

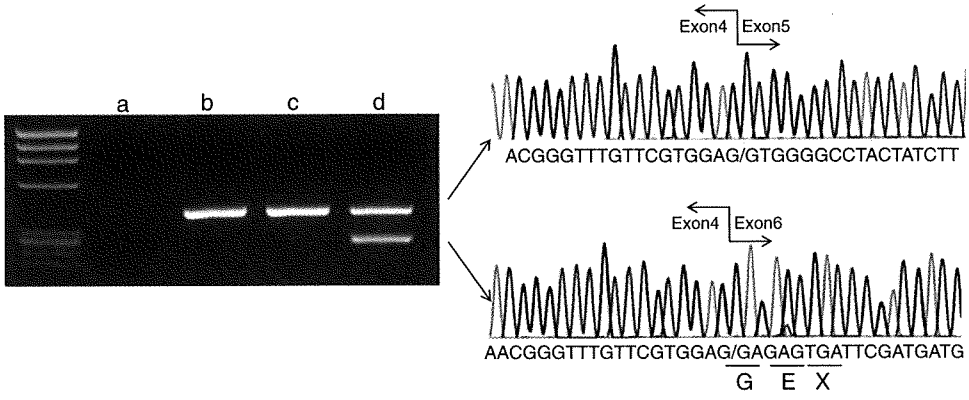

Fig. 3 Transcript abnormality in the SLC12A1 gene. Electrophoresis and the direct sequencing results of cDNA after PCR. The control leukocyte sample shows no band **a**, the control kidney **b** and urine sediments **c** samples show only one normal band, whereas the sample extracted from urinary sediments of the patient **d** show two bands, one the same size as the control sample and the other show an exon 5 skipped sequence

type I BS. These mutations include missense, nonsense, deletion, insertion, and splicing site mutations as well as intronic mutations outside the splice consensus sequence (Simon et al. 1996; Vargas-Poussou et al. 1998; Brochard et al. 2009). However, the biological effect of missense mutations or intronic alterations outside the splice consensus site is often difficult to assess without further functional analysis. For missense mutations, biophysiological functional analysis is usually performed to determine whether the mutation is disease associated. On the other hand, to identify intronic mutations resulting in aberrant splicing is difficult because target tissues other than peripheral blood leukocytes are not always available for the mRNA analysis. Furthermore, alternative splicing is frequently observed in truncation and when exon skipping is observed, it is difficult to determine whether it is a disease-causing splicing abnormality. Therefore, functional splicing study is needed for the intronic mutations.

In the study reported here, a novel compound heterozygous mutation of c.724 + 4A > G and c.2095delG of the *SLC12A1* gene was identified in a Japanese girl diagnosed with antenatal BS. However, it was not clear whether the former was a mutation that could be the pathogenic for type I BS. In fact, this intronic mutation was not detected in 100 healthy control samples and the Shapiro's splicing probability scores for the splice donor site of intron 5 were therefore calculated (Shapiro and Senapathy 1987). The scores for the intron 5 splice donor site were 0.86 for the wild type and 0.74 for the mutant, leading to a strong suspicion that the splicing donor site was disrupted with this mutation. For this reason, we conducted in vivo and in vitro splicing assays to resolve this problem.

First, we performed the in vivo splicing analysis using urinary sediments. It is important to identify transcript abnormalities in every target organ, and only when transcripts were expressed in the blood leukocytes, could we conduct our investigation at the transcript level using the leukocytes instead. However, the transcripts of the *SLC12A1* gene were not expressed in blood leukocytes (Fig. 3). Renal biopsy specimens can be used as a source for mRNA analysis in inherited kidney diseases, but renal biopsy is invasive and not always needed for some kidney diseases including BS. Urinary sediments, on the other hand, contain cells derived from the kidney, and genetic analysis using those cells constitutes an entirely non-invasive, simple method for the diagnosis of inherited kidney diseases. Igarashi et al. were the first to identify transcript abnormalities by extracting mRNA from urinary sediment cells of patients with Dent disease (Igarashi et al. 2000). Following up on this result, we used this analytical method for two inherited kidney diseases, Gitelman syndrome and Alport syndrome, and both analyses were successful (Iida et al. 2008; Kaito et al. 2007; Krol et al. 2008). However, since in these three diseases (Dent disease, Gitelman syndrome and Alport syndrome) the mRNA of the causative genes is also expressed in the leukocytes a transcriptional study using leukocytes could be used as an alternative. The mRNA of the *SLC12A1* gene was not detected in the leukocytes demonstrating that this in vivo assay is quite useful for all inherited kidney diseases to determine the presence of abnormal transcripts in target organ cells.

Second, we performed in vitro splicing analysis by using a hybrid minigene which clearly showed the intronic mutation disrupt splice donor site. This finding indicated that the c.724 + 4A > G mutation was likely to be the pathogenic mutation for type I BS. In vitro splicing assays have been conducted for several diseases to identify the splicing abnormalities derived from intronic and sometimes exonic mutations (Thi Tran et al. 2005; Tran et al. 2006; Takeshima et al. 1995; Tran et al. 2007). For inherited kidney diseases, Bergmann et al. conducted a splicing analysis to confirm whether the *PKHD1* c.53-3C > A in intron 2 mutation leads to exon 3 skipping in the transcripts (Bergmann et al. 2006). They used this analysis because they could not get mRNA from kidney specimens and proved that this mutation was disease causing. In our study, however, we obtained the same proof both in vivo and in vitro by using urinary sediments and minigene construction, thus confirming the both methods are sufficiently reliable.

The results of our in vitro splicing assay of the minigene encoding the wild-type exon 5 unfortunately showed a certain quantity of the product without exon 5 in both HeLa and HEK293 cell lines. We confirmed that the transcripts with exon 5 skipped were negative in normal kidney and normal urine sediments cDNA, which means exon 5 was not alternatively spliced in the normal transcripts. To explore the effect of the exonic splicing silencers (ESS) on exon 5 (Wang et al. 2004), the web-based resources known as ACESCAN2 (ACESCAN2 Web Server, http://genes.mit.edu/acescan2/index.html) were used to identify putative ESS and it became clear that there are 12 candidate sequences for ESS in exon 5. It is speculated that these sequences caused exon skipping in this in vitro assay. Another consideration is that, although previous reports using the same minigene construction showed clear results (Thi Tran et al. 2005; Tran et al. 2006; Takeshima et al. 1995; Tran et al. 2007), this assay has limited splicing ability, which sometimes leads to incomplete results as reported here.

According to the parents, the patient's elder sister who was prematurely born under condition of polyhydramnios died as an infant because of severe infection. Although no medical record could be obtained, we speculate she probably died not from severe infection and septic shock but from hypovolemic shock due to the same inherited tubulopathy.

Our in vivo and in vitro assays clearly proved the c.724 + 4A > G mutation is the pathogenic mutation for type I BS. To the best of our knowledge, this is the first study to demonstrate the efficacy of the non-invasive in vivo and in vitro functional splicing assays for Bartter syndrome. These analytical assays have the potential to be adapted to all inherited kidney diseases where patients' genetic tests show the presence of intronic mutations that are strongly suspected of being pathogenic.

Acknowledgments This work is supported by A Grant in Aid for Young Scientists (B-19790720) (to K. N.) from the Japan Society for the Promotion of Science.

References

Bergmann C, Frank V, Kupper F et al (2006) Functional analysis of PKHD1 splicing in autosomal recessive polycystic kidney disease. J Hum Genet 51(9):788–793

Birkenhager R, Otto E, Schurmann MJ et al (2001) Mutation of BSND causes Bartter syndrome with sensorineural deafness and kidney failure. Nat Genet 29(3):310–314

Brochard K, Boyer O, Blanchard A, et al (2009) Phenotype–genotype correlation in antenatal and neonatal variants of Bartter syndrome. Nephrol Dial Transplant 24(5):1455–1464

Igarashi T, Inatomi J, Ohara T et al (2000) Clinical and genetic studies of CLCN5 mutations in Japanese families with Dent's disease. Kidney Int 58(2):520–527

Iida K, Nozu K, Takahashi Y et al (2008) Characterization of a splicing abnormality in Gitelman syndrome. Am J Kidney Dis 51(6):1077–1078

Kaito H, Nozu K, Fu XJ et al (2007) Detection of a transcript abnormality in mRNA of the SLC12A3 gene extracted from urinary sediment cells of a patient with Gitelman's syndrome. Pediatr Res 61(4):502–505

Krol RP, Nozu K, Nakanishi K et al (2008) Somatic mosaicism for a mutation of the COL4A5 gene is a cause of mild phenotype male Alport syndrome. Nephrol Dial Transplant 23(8):2525–2530

Shapiro MB, Senapathy P (1987) RNA splice junctions of different classes of eukaryotes: sequence statistics and functional implications in gene expression. Nucleic Acids Res 15(17):7155–7174

Simon DB, Karet FE, Hamdan JM et al (1996a) Bartter's syndrome, hypokalaemic alkalosis with hypercalciuria, is caused by mutations in the Na–K–2Cl cotransporter NKCC2. Nat Genet 13(2):183–188

Simon DB, Karet FE, Rodriguez-Soriano J et al (1996b) Genetic heterogeneity of Bartter's syndrome revealed by mutations in the K+ channel, ROMK. Nat Genet 14(2):152–156

Simon DB, Bindra RS, Mansfield TA et al (1997) Mutations in the chloride channel gene, CLCNKB, cause Bartter's syndrome type III. Nat Genet 17(2):171–178

Takeshima Y, Nishio H, Sakamoto H et al (1995) Modulation of in vitro splicing of the upstream intron by modifying an intra-exon sequence which is deleted from the dystrophin gene in dystrophin Kobe. J Clin Invest 95(2):515–520

Thi Tran HT, Takeshima Y, Surono A et al (2005) A G-to-A transition at the fifth position of intron-32 of the dystrophin gene inactivates a splice-donor site both in vivo and in vitro. Mol Genet Metab 85(3):213–219

Tran VK, Takeshima Y, Zhang Z et al (2006) Splicing analysis disclosed a determinant single nucleotide for exon skipping caused by a novel intraexonic four-nucleotide deletion in the dystrophin gene. J Med Genet 43(12):924–930

Tran VK, Takeshima Y, Zhang Z et al (2007) A nonsense mutation-created intraexonic splice site is active in the lymphocytes, but not in the skeletal muscle of a DMD patient. Hum Genet 120(5):737–742

Vargas-Poussou R, Feldmann D, Vollmer M et al (1998) Novel molecular variants of the Na–K–2Cl cotransporter gene are responsible for antenatal Bartter syndrome. Am J Hum Genet 62(6):1332–1340

Wang Z, Rolish ME, Yeo G et al (2004) Systematic identification and analysis of exonic splicing silencers. Cell 119(6):831–845

Pediatr Nephrol (2009) 24:1071–1075
DOI 10.1007/s00467-008-1044-2

BRIEF REPORT

Increased chymase-positive mast cells in children with crescentic glomerulonephritis

Hiroko Togawa · Koichi Nakanishi · Yuko Shima · Mina Obana · Mayumi Sako · Kandai Nozu · Ryojiro Tanaka · Kazumoto Iijima · Norishige Yoshikawa

Received: 11 August 2008 / Revised: 14 October 2008 / Accepted: 15 October 2008 / Published online: 3 December 2008

Abstract Mast cell-derived chymase is an angiotensin II-forming enzyme that appears to be involved in tubulointerstitial fibrosis in the kidneys. Previous studies have shown that the level of chymase increases in grafted kidneys after rejection and in adult patients with diabetic nephropathy. However, the significance of chymase in children with renal diseases has not been investigated. Using immunohistochemistry, we have investigated chymase expression in biopsy samples of renal tissue from 104 children with kidney diseases, including rapidly progressive crescentic glomerulonephritis (n=3), diabetic nephropathy (n=2), allografted kidney (n=3), membranoproliferative glomerulonephritis (n=6), immunoglobulin A nephropathy (n=33) and Henoch–Schönlein purpura nephritis (n=23). Increased numbers of chymase-positive mast cells were observed in the renal cortex of all three patients with crescentic glomerulonephritis (mean 26.0/mm^2; range 19.3–36.8/mm^2). Chymase-positive cells were also observed in the renal biopsy of an allografted kidney and in those from children with diabetic nephropathy. The mean number of chymase-positive cells in renal tissue samples characterized by each renal disease was significantly correlated with the mean intensity of the interstitial fibrosis in that same tissue sample (Spearman's rank correlation test p=0.0013; rank correlation coefficient 0.84). These findings suggest that mast cell-derived chymase plays an important role in juvenile crescentic glomerulonephritis.

Keywords Angiotensin II · Diabetic nephropathy · Allografted kidney · Immunohistochemistry · Immunoglobulin A nephropathy · Interstitial fibrosis · Rapidly progressive glomerulonephritis

H. Togawa · K. Nakanishi (✉) · Y. Shima · M. Obana · M. Sako · N. Yoshikawa
Department of Pediatrics, Wakayama Medical University,
811-1 Kimiidera,
Wakayama City, Wakayama 641-8509, Japan
e-mail: knakanis@wakayama-med.ac.jp

K. Nozu · K. Iijima
Department of Pediatrics,
Kobe University Graduate School of Medicine,
Kobe, Hyogo, Japan

R. Tanaka
Department of Nephrology,
Hyogo Prefectural Kobe Children's Hospital,
Kobe, Hyogo, Japan

Introduction

Mast cell (MC)-derived chymase is one of the serine proteases present in the secretory granules of MCs. It is an angiotensin II (ATII)-forming enzyme, similar to angiotensin converting enzyme (ACE). Chymase has no enzymatic activity under normal physiological conditions, but it is activated immediately after release into the extracellular matrix. Unlike ACE, the effects of chymase are limited to specific tissues. It has been suggested that chymase plays an important role in the progression of tubulointerstitial fibrosis via ATII. Recent studies have shown that chymase expression increases in rejected kidney grafts and in the kidneys of adults with diabetic nephropathy and immunoglobulin A nephropathy (IgAN) [1–4]. To date, however, the significance of chymase in children with renal diseases is still unclear.

Methods

Patients

Biopsy samples of renal tissue from 104 pediatric patients with renal diseases were examined (Table 1). The mean patient age± standard deviation (SD) was 10.6±4.9 years, and there was an equal distribution of sexes (52:52) in the patient cohort. Each renal specimen was subjected to routine histological examination, and the intensity of interstitial fibrosis was graded semiquantitatively based on the Banff classification of renal allograft pathology (from ci0 to ci3) [5]. A summary of three patients with crescentic glomerulonephritis showing rapidly progressive glomerulonephritis (RPGN) clinically is shown in Table 2. The estimated glomerular filtration rates (eGFRs) at renal biopsy by Schwartz's formula were 22.0, 8.8 and 7.6 ml/min per 1.73 m^2 body surface area (BSA). All of the patients with other renal diseases, except for those with allografted kidneys, showed normal eGFR (≥90 ml/min per 1.73 m^2 BSA). Of the patients with allografted kidneys, two underwent protocol biopsies (1 and 3 years after renal transplantation, respectively) and one underwent an event biopsy. Their eGFRs were 85.9 (1 year), 75.3 (3 years) and 11.6 (event) ml/min per 1.73 m^2 BSA, respectively. With IgAN, the extent of mesangial proliferation (focal or diffuse) was defined based on World Health Organization criteria [6]. Henoch–Schönlein purpura nephritis (HSPN) was graded using the International Study of Kidney Disease of Children's (ISKDC) grade [7]. Each patient's family gave informed consent for the renal biopsy and studies.

Immunohistochemical staining

Samples of biopsied kidney were snap-frozen and stored at −80°C until use, at which time they were then cut into 4-μm-thick sections using a cryostat and subjected to immunohistochemical staining. The sections were fixed in Carnoy's fixative before staining for chymase, which involved incubation with anti-human chymase monoclonal antibody (diluted 1:500; Chemicon International, Temecula, CA) for 1 h at room temperature. After washing, the

Table 1 Mast cell chymase expression in kidney tissues from children with various renal diseases

Diagnosis	Number of patients	Mean intensity of interstitial fibrosis[a, b] (range)	Number of patients showing chymase-positive cells (%)	Mean number of chymase-positive cells[b]/mm^2 (range)
Crescentic glomerulonephritis	3	3.0 (3–3)	3 (100.0%)	26.0 (19.3–36.8)
Diabetic nephropathy	2	0.5 (0–1)	1 (50.0%)	2.6 (0–5.1)
Allografted kidney	3	0.7 (0–1)	1 (33.3%)	2.2 (0–6.5)
Protocol biopsy	2	0.5 (1–1)	0 (0.0%)	0.0 (0–0)
Event biopsy	1	0.0	1 (100.0%)	6.5
Membranoproliferative glomerulonephritis	6	0.2 (0–1)	2 (33.3%)	0.5 (0–2.4)
Immunoglobulin A nephropathy	33	0.3 (0–2)	6 (18.2%)	0.6 (0–7.0)
Focal mesangial proliferation	22	0.1 (0–1)	4 (18.2%)	0.4 (0–2.4)
Diffuse mesangial proliferation	11	0.6 (0–2)	2 (18.2%)	0.9 (0–7.0)
Focal segmental glomerulosclerosis	6	1.2 (1–2)	1 (16.7%)	0.3 (0–1.9)
Henoch–Schönlein purpura nephritis	23	0.3 (0–2)	2 (8.7%)	0.3 (0–6.2)
Crescent < 50%	16	0.1 (0–1)	2 (12.4%)	0.4 (0–6.2)
Crescent ≥ 50%	7	0.7 (0–2)	0 (0.0%)	0.0 (0–0)
Minimal-change nephrotic syndrome	22	0.0 (0–0)	1 (4.6%)	0.1 (0–1.1)
Membranous glomerulonephritis	3	0.0 (0–0)	0 (0.0%)	0.0 (0–0)
Alport's syndrome	2	0.0 (0–0)	0 (0.0%)	0.0 (0–0)
Lupus nephritis, Class IV-G (A)	1	0.0	0 (0.0%)	0.0

[a] The intensity of interstitial fibrosis was graded semiquantitatively using the Banff classification of renal allograft pathology (from ci0 to ci3) [5]
[b] Spearman's rank correlation test showed that the p value and rank correlation coefficient were 0.0013 and 0.84 between them

Table 2 Crescentic glomerulonephritis showing rapidly progressive glomerulonephritis syndrome

Case number	Sex of patient	Age at biopsy (years)	Duration from detection to biopsy (days)	eGFR by Schwartz's formula at biopsy (ml/min per 1.73 m^2)	ANCA	Anti-GBM antibody	Circulating immune complex	Interstitial fibrosis[a]	Number of chymase-positive cells (/mm^2)
1	M	8	11	22.0	MPO+ PR3−	−	−	3+	36.8
2	F	6	20	8.8	MPO+ PR3−	N/D	−	3+	21.8
3	M	10	11	7.6	MPO− PR3−	−	−	3+	19.3

eGFR Estimated glomerular filtration rate; *ANCA* anti-neutrophil cytoplasmic antibody; *PR3* proteinase-3; *MPO* myeloperoxidase; *GBM* glomerular basement membrane; *N/D* not determined

[a] The intensity of interstitial fibrosis was graded semiquantitatively on a scale from 0 to 3+: none, 0; slight, 1+; moderate, 2+; and intense, 3+

sections were incubated with a secondary antibody conjugated to a peroxidase-labeled polymer using the Envision+ system (Dako Cytomation, Glostrup, Denmark). These samples were visualized with 3,3′-diaminobenzidine tetrahydrochloride and counterstained with hematoxylin. A double staining procedure using rabbit anti-human CD117 (c-kit) antibody (diluted to 1:400; Dako Cytomation) was performed to confirm that the chymase-positive cells were MCs. For negative control staining, we used the vehicle or the secondary antibody alone.

Counting of chymase-positive cells

All chymase-positive cells in the whole area of each section were counted, and the area of each section was measured using Image J ver. 1.37 software (National Institutes of Health, Bethesda, MD). This was performed blind, without knowledge of the clinical and pathological findings. The number of positively stained cells in each section was expressed as the absolute number of positive cells per square millimeter.

Statistical analyses

Spearman's rank correlation test was used to examine the association between the mean intensity of interstitial fibrosis and the mean number of chymase-positive cells of each renal disease.

Results

The number of patients examined, the mean intensity of interstitial fibrosis, the number and ratio of patients showing chymase-positive cells and the mean number of chymase-positive cells per square millimeter are shown in Table 1. Chymase expression was observed only in the interstitium.

Chymase expression was detected in the tissue samples of all three patients with crescentic glomerulonephritis. A representative micrograph showing chymase expression in renal tissue from a patient with crescentic glomerulonephritis is shown in Fig. 1. The mean number of chymase-positive cells in the renal cortex of these patients was 26.0/mm^2 (range 19.3–36.8). The renal specimens from all of the children with crescentic glomerulonephritis showed intense interstitial fibrosis.

The mean numbers of chymase-positive cells were 5.1 and 6.5/mm^2, respectively, in those patients with diabetic nephropathy and with allografted kidneys showing positive chymase expression (one patient each). The renal specimen from the patient with diabetic nephropathy with chymase-positive cells showed slight interstitial fibrosis, while that without chymase-positive cells showed no interstitial

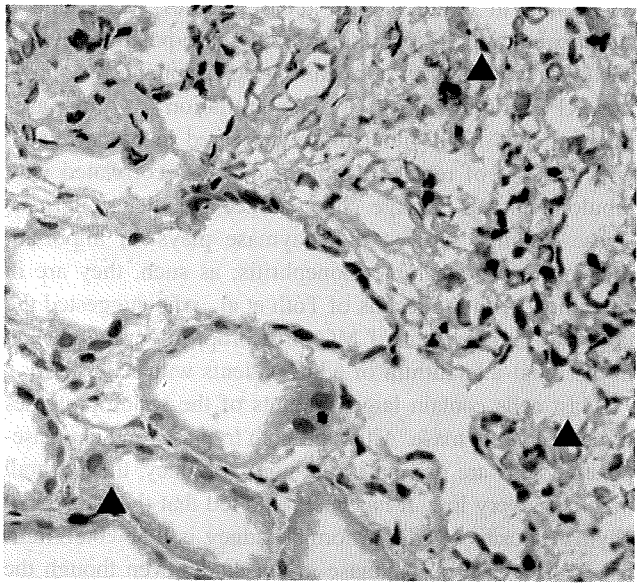

Fig. 1 A representative micrograph showing chymase expression in renal tissue from a patient with crescentic glomerulonephritis. *Arrowheads* Chymase-positive cells

fibrosis. The patient with an allografted kidney showing positive chymase expression underwent an event renal biopsy, which demonstrated acute tubule necrosis.

In tissue samples obtained from patients with membranoproliferative glomerulonephritis, the maximum number of chymase-positive cells was 2.4/mm^2. In those from patients with IgAN, there was no difference in the chymase-positive cell ratio between focal and diffuse mesangial proliferation. The maximum numbers of chymase-positive cells were 2.4 and 7.0/mm^2 in renal tissue samples showing focal and diffuse mesangial proliferation, respectively.

One patient of the six children with focal segmental glomerulosclerosis (16.7%) and one of the 22 with minimal-change nephrotic syndrome (4.6%) showed chymase positive cells.

Among the 23 HSPN patients, two showed chymase-positive cells. There was no association between ISKDC grade and chymase-positive cell ratio in HSPN.

The mean number of chymase-positive cells in tissue samples characterized by each renal disease was significantly correlated with the mean intensity of the interstitial fibrosis in that same tissue sample (Spearman's rank correlation test p=0.0013; rank correlation coefficient 0.84).

Discussion

The aim of this study was to clarify the involvement of MC-derived chymase in children with renal diseases. To our knowledge, this is the first report to describe chymase expression in children with renal diseases. We found a significantly increased number of chymase-positive MCs in all three patients with crescentic glomerulonephritis showing RPGN clinically. The accumulation of chymase-positive cells in the interstitium appeared to be correlated with the loss of renal function, and it was correlated with tubulointerstitial damage characterized by intense fibrosis. These findings suggest that chymase plays an important role in crescentic glomerulonephritis; as such, they are in agreement with the results of Tóth et al., who suggested the potential involvement of MCs in fibroproliferative change in the renal interstitium of adult patients with RPGN [8].

Mast cells contain large amounts of the serine proteases tryptase and chymase. Although both tryptase- and chymase-positive cells are present in the normal kidney, their overall number is very low. It has been reported that the number of chymase-positive cells in normal kidney is 0.58±0.38/mm^2 [1]. We focused on chymase in our study, even though the number of tryptase-positive cells is reportedly double that of cells positive for chymase [1] because of the ATII-generating property of that latter serine protease.

It has also been reported that the number of chymase-positive cells in rejected kidneys is positively correlated with the degree of fibrosis [1]. In our study, an event biopsy of one allografted kidney with acute tubule necrosis and no rejection showed an increased number of chymase-positive cells (6.5/mm^2). This finding suggests that chymase may play a role in acute tubule necrosis of allografted kidneys.

Huang et al. reported a markedly increased chymase expression associated with severe pathological changes in the kidneys of patients with diabetic nephropathy [3]. With the exception of mild tubulointerstitial fibrosis, no such findings were evident in our patients with diabetic nephropathy. The reason for this difference is unclear, but disease severity may have been partly responsible.

Studies in adult patients with IgAN suggest that MC-derived chymase plays a role in the progression of IgAN [4, 9]. However, in our population of children with IgAN, the findings suggest that chymase does not play a major role, perhaps because of a difference in disease progression level between children and adults. Interestingly, glomerular hypercellularity in the mesangial area is more prominent in children than in adults, while, in contrast, glomerular matrix expansion, crescent formation and interstitial damage are more severe in adults than in children [10]. These histological differences may be related to chymase expression patterns.

It is unknown whether chymase plays a disease-specific role in crescentic glomerulonephritis. In most of the children with renal diseases in our series, renal biopsy specimens did not show fibrosis. This may be the main reason why the numbers of chymase-positive cells were not so high in most of the diseased tissue samples we studied.

Although an increase of chymase is usually interpreted as a sign of pathological involvement, recent data have suggested that it can restore kidney homeostasis [11]. It has been reported that chymase regulates the activities of pro-matrix metalloprotease (MMP)-2 and -9 [12].

It has been demonstrated that at least 40% of angiotensin I can be converted to ATII by a pathway other than ACE in the normal kidney [13]. Although the effect of chymase inhibitors in renal diseases has not yet been investigated, they may have potency as renoprotective agents.

In conclusion, the findings of our study suggest that MC-derived chymase plays a pivotal role in disease progression in children with crescentic glomerulonephritis showing RPGN. However, the number of patients we investigated was very small, and additional analysis will be required to establish the role of chymase in children with kidney diseases.

Acknowledgments This study was presented at the 51st Annual Meeting of Japanese Society of Nephrology, Fukuoka, Japan, 2008.

References

1. Yamada M, Ueda M, Naruko T, Tanabe S, Han YS, Ikura Y, Ogami M, Takai S, Miyazaki M (2001) Mast cell chymase expression and mast cell phenotypes in human rejected kidneys. Kidney Int 59:1374–1381
2. Ritz E (2003) Chymase: a potential culprit in diabetic nephropathy? J Am Soc Nephrol 14:1738–1747
3. Huang XR, Chen WY, Truong LD, Lan HY (2003) Chymase is upregulated in diabetic nephropathy: implications for an alternative pathway of angiotensin II-mediated diabetic renal and vascular disease. J Am Soc Nephrol 14:1738–1747
4. Miyake-Ogawa C, Miyazaki M, Abe K, Harada T, Ozono Y, Sakai H, Koji T, Kohno S (2005) Tissue-specific expression of renin-angiotensin system components in IgA nephropathy. Am J Nephrol 25:1–12
5. Racusen LC, Solez K, Colvin RB, Bonsib SM, Castro MC, Cavallo T, Croker BP, Demetris AJ, Drachenberg CB, Fogo AB, Furness P, Gaber LW, Gibson IW, Glotz D, Goldberg JC, Grande J, Halloran PF, Hansen HE, Hartley B, Hayry PJ, Hill CM, Hoffman EO, Hunsicker LG, Lindblad AS, Marcussen N, Mihatsch MJ, Nadasdy T, Nickerson P, Olsen ST, Papadimitriou JC, Randhawa PS, Rayner DC, Roberts I, Rose S, Rush D, Salinas-Madrigal L, Salomon DR, Sund S, Taskinen E, Trpkiv K, Yamaguchi Y (1999) The Banff 97 working classification of renal allograft pathology. Kidney Int 55:713–723
6. Churg J, Bernstein J, Glassock RJ (1995) Renal disease: classification and atlas of glomerular diseases, 2nd edn. Igaku-shoin Medical Publishers Tokyo
7. Yoshikawa N, Nakanishi K, Iijima K (2001) Henoch-Schönlein purpura. In: Neilson EG, Couser WG (eds) Immunologic renal diseases, 2nd edn. Lippincott Williams & Wilkins, Philadelphia, pp 1127–1140
8. Tóth T, Tóth-Jakatics R, Jimi S, Ihara M, Urata H, Takebayashi S (1999) Mast cells in rapidly progressive glomerulonephritis. J Am Soc Nephrol 10:1498–1505
9. Ehara T, Shigematsu H (1998) Contribution of mast cells to the tubulointerstitial lesions in IgA nephritis. Kidney Int 54:1675–1683
10. Ikezumi Y, Suzuki T, Imai N, Ueno M, Narita I, Kawachi H, Shimizu F, Nikolic-Paterson DJ, Uchiyama M (2006) Histological differences in new-onset IgA nephropathy between children and adults. Nephrol Dial Transplant 21:3466–3474
11. Blank U, Essig M, Scandiuzzi L, Benhamou M, Kanamaru Y (2007) Mast cells and inflammatory kidney disease. Immunol Rev 217:79–95
12. Tchougounova E, Lundequist A, Fajardo I, Winberg JO, Abrink M, Pejler G (2005) A key role for mast cell chymase in the activation of pro-matrix metalloprotease-9 and pro-matrix metalloprotease-2. J Biol Chem 280:9291–9296
13. Hollenberg NK, Fisher ND, Price DA (1998) Pathways for angiotensin II generation in intact human tissue: evidence from comparative pharmacological interruption of the renin system. Hypertension 32:387–392

0031-3998/09/6605-0590
PEDIATRIC RESEARCH

Vol. 66, No. 5, 2009
Printed in U.S.A.

A Deep Intronic Mutation in the *SLC12A3* Gene Leads to Gitelman Syndrome

KANDAI NOZU, KAZUMOTO IIJIMA, YOSHIMI NOZU, EI IKEGAMI, TAKEHIDE IMAI, XUE JUN FU, HIROSHI KAITO, KOICHI NAKANISHI, NORISHIGE YOSHIKAWA, AND MASAFUMI MATSUO

Department of Pediatrics [K.N., K.I., Y.N., X.J.F., H.K., M.M.], Kobe University Graduate School of Medicine, Kobe, Hyogo 6500017, Japan; Department of Pediatrics [E.I., T.I.], Nippon Medical School, Tokyo 1138602, Japan; Department of Pediatrics [K.N., N.Y.], Wakayama Medical University, Wakayama 6418509, Japan

ABSTRACT: Many mutations have been detected in the *SLC12A3* gene of Gitelman syndrome (GS, OMIM 263800) patients. In previous studies, only one mutant allele was detected in ~20 to 41% of patients with GS; however, the exact reason for the nonidentification has not been established. In this study, we used RT-PCR using mRNA to investigate for the first time transcript abnormalities caused by deep intronic mutation. Direct sequencing analysis of leukocyte DNA identified one base insertion in exon 6 (c.818_819insG), but no mutation was detected in another allele. We analyzed RNA extracted from leukocytes and urine sediments and detected unknown sequence containing 238bp between exons 13 and 14. The genomic DNA analysis of intron 13 revealed a single-base substitution (c.1670–191C>T) that creates a new donor splice site within the intron resulting in the inclusion of a novel cryptic exon in mRNA. This is the first report of creation of a splice site by a deep intronic single-nucleotide change in GS and the first report to detect the onset mechanism in a patient with GS and missing mutation in one allele. This molecular onset mechanism may partly explain the poor success rate of mutation detection in both alleles of patients with GS. ***(Pediatr Res* 66: 590–593, 2009)**

Gitelman syndrome (GS, OMIM 263800) is an autosomal recessive renal disorder characterized by hypokalemia, hypomagnesemia, metabolic alkalosis, and hypocalciuria (1). Mild weakness, cramps, and general fatigue are clinically observable, but they are often so slight that patients with GS are not diagnosed until late childhood or even adulthood; however, a reduced health quality of life for patients with GS, compared with a control group, has been referred (2). Simon *et al.* (3) demonstrated that mutations in the *SLC12A3* gene encoding the thiazide-sensitive sodium-chloride cotransporter (NCCT) are responsible for GS. This gene, which is located in chromosome 16 and comprises 26 exons, is a 1021-amino acid protein with 12 predicted transmembrane domains. The lack of a functional NCCT leads to a decrease in sodium and chloride reabsorption in the distal convoluted tubule and an increase in solute delivery to the collecting duct. These changes result in blood volume reduction, activation of the renin-angiotensin-aldosterone system, and increased secretion of potassium and hydrogen ions into the collecting duct.

To date, >100 different mutations throughout the *SLC12A3* gene have been identified in patients with GS, but only one mutant allele was detected in ~20 to 41% of patients with GS (3–7). However, the exact reason for the nonidentification has not been established.

This report concerns a patient with GS and only one mutation in the exons and exon-intron boundaries. However, we succeeded in detecting a deep intronic mutation that creates a new donor splice site resulting in the inclusion of a novel cryptic exon in mRNA. This novel disease onset mechanism may partly explain the poor success rate of mutation detection in both alleles in patients with GS and how single-base changes deep within introns can cause GS.

PATIENTS AND METHODS

Case report. The subject of this study was a 12-y-old girl who was suffering from paralysis, muscle stiffness, and pain. When she was referred to our hospital, a blood examination disclosed that her serum potassium level was low. No medicine, such as diuretics or laxatives, had been prescribed previously. On admission, she was 145-cm tall (−2.5 SD), weighed 46 kg, her blood pressure was 102/62 mm Hg, and physical examination findings were normal. Laboratory results showed that serum potassium was low (1.9 mEq/L; normal: 3.5–4.7 mEq/L), whereas plasma renin activity (20 pg mL^{-1} h^{-1}; normal: 0.2–3.9 ng mL^{-1} h^{-1}) and aldosterone concentration (297 pg/mL; normal: 29.9–159 pg/mL) were elevated. Serum magnesium (1.4–1.6 mg/dL; normal: 1.7–2.5 mg/dL), and urinary calcium (urine calcium/creatinine: 0.02) and chloride excretion (FeCl 0.88%; normal: 1.6–3.2%) were also low. Her parents were nonconsanguineous.

This study was approved by the Institutional Review Board of Kobe University Graduate School of Medicine and consent for this study was obtained from the patient's parents.

Genetic analyses. Genomic DNA was isolated from peripheral blood leukocytes of the patient as well as from normal control subjects with the Qiagen kit (Qiagen Inc., Chatsworth, CA), according to the manufacturer's instructions. Primer pairs for the *SLC12A3* gene and the *CLCNKB* gene were generated following previous reports (8,9). Polymerase chain reaction (PCR) was performed and the resultant products were analyzed, including every intron-exon boundary, by direct sequencing with a DNA sequencer (Perkin-Elmer-ABI, Foster City, CA). Multiplex ligation-dependent probe amplification (MLPA) was also conducted by means of the SALSA P136-Gitelman MLPA assay (MRC-Holland, Amsterdam, The Netherlands) and following the manufacturer's instructions.

Total RNA was extracted from blood leukocytes and urine sediments. The urine sediments were obtained by centrifugation at 1500 × *g* for 10 min from

Received May 20, 2009; accepted July 1, 2009.
Correspondence: Kandai Nozu, M.D., Ph.D., Department of Pediatrics, Kobe University Graduate School of Medicine, Kusunoki-cho 7-5-1, Chuo-ku, Kobe, Hyogo 6500017, Japan; e-mail: nozu@med.kobe-u.ac.jp
Supported by Grant in Aid (B-19790720) (to K.N.) from the Japan Society for the Promotion of Science.

Abbreviations: GS, Gitelman syndrome; **MLPA,** multiplex ligation-dependent probe amplification

100 mL of early morning urine. Microscopic examination of these sediments confirmed that they contained sufficient renal tubular epithelial cells having large round nucleus surrounded by a large granular cytoplasm which is larger than granulocytes (10). RNA was isolated with the aid of Isogen Kit (Nippon Gene Co., Toyama, Japan) and was then reverse-transcribed onto cDNA by using random hexamers and the Superscript III kit (Invitrogen). cDNA was amplified by means of nested PCR using primer pairs. The primer sequences of exons 13 to 15 were as follows: exon13, first forward: GTACCCACT-GATCGGCTTCT; second forward: TTCCTCTGCTCCTATGCC; exon 15, first reverse: TCCTCGGCAATGACATCC; second reverse: GGGCGG-TAGTTCTTGATGT. After 40 cycles of amplification, PCR products were separated on 2% agarose and sequenced with a DNA sequencer (Perkin-Elmer-ABI, Foster City, CA). For sequencing, amplified products were separated by electrophoresis, and the RT-PCR products were purified. The purified products were subcloned into pT7 vector (Novagen, Inc., Madison, WI), and the inserted products were sequenced. Normal control kidney cDNA was obtained from the Human Kidney cDNA Library (Invitrogen). Normal control blood leukocytes and urinary sediments samples were obtained from a healthy control to extract total RNA.

RESULTS

Direct sequencing of the PCR-amplified products disclosed a novel heterozygous single-base insertion of G between nucleotides 818 and 819 in exon 6. This mutation was also seen in the father's genomic DNA (Fig. 1*A*). Because the second abnormality was not detectable, we conducted an MLPA analysis using the MLPA kit for GS. However, no large heterozygous deletion was detected with this approach, either. Next, we performed a complete transcript sequence analysis using mRNA extracted from leukocytes. In addition to the normal band in the fragment of exons 13 to 15, an abnormal band was detected in the RT-PCR products from the patient's sample, which showed two bands, one the same size as the control and the other larger (Fig. 2). After subcloning of the two bands, sequencing was conducted, and the larger product disclosed a normal sequence containing a 238-bp insertion between exons 13 and 14, which are part of intron 13 (Figs. 1*B* and 3). This insertion was not detected in cDNA from a normal blood leukocytes, kidney, and urinary sediments (Fig. 2). To shed light on the mechanism involved in this intronic sequence exonization, we sequenced this part of intron 13 and identified the c.1670–191C>T heterozygous base substitution at the position immediately after the insertion sequence and created a novel splicing donor site for cryptic exon resulting in the 238-bp insertion in the mRNA (Fig. 4). This mutation was found in the genomic DNA of both the patient and the mother (Fig. 1C), whereas not detected in 100 normal control samples (200 chromosomes). Moreover, no mutations were detected in the *CLCNKB* gene. It was thus demonstrated that this patient possessed a compound heterozygous mutation of c.818_819insG and c.1670–191C>T and the GS phenotype. Both mutations will lead to

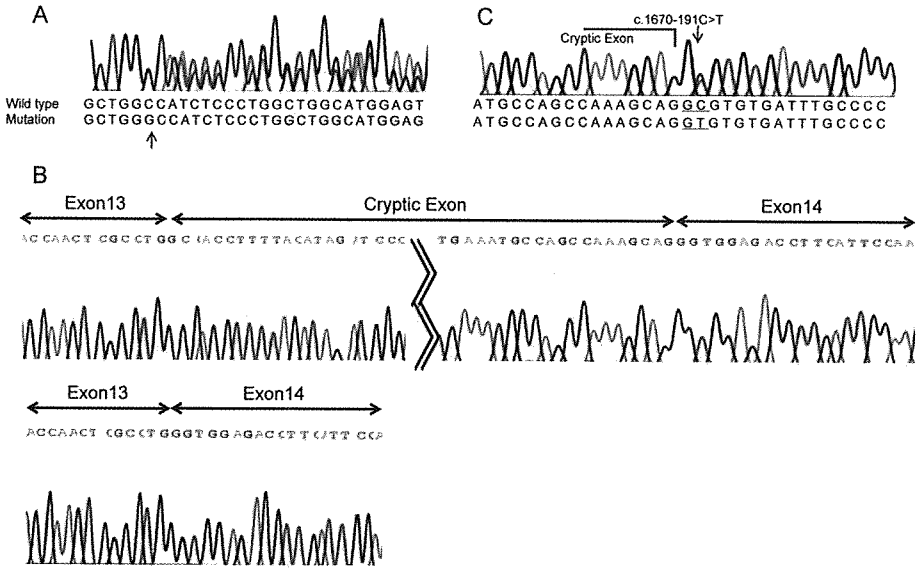

Figure 1. Nucleotide changes in the *SLC12A3* gene. *A*, A heterozygous 1-bp insertion between nucleotides 818 and 819 located in exon 6 (c.818_819insG) was detected in the paternal allele. *B*, Fragments of the sequence after subcloning of the sense strand of cDNA from the patient. The larger product (upper figure) containing 238-bp cryptic exon sequence and the smaller product (lower figure) showed the normal sequence. *C*, A heterozygous single-base substitution of C to T in intron 13 (c.1670-191C>T) was detected in the maternal allele.

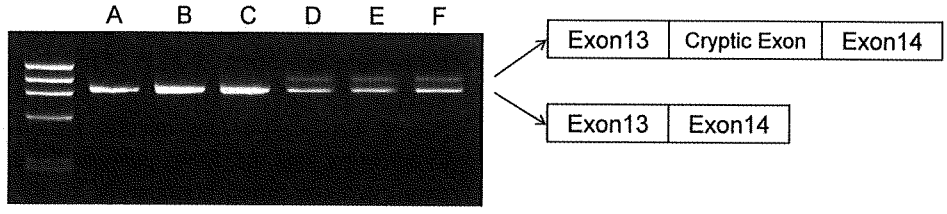

Figure 2. A transcript abnormality in the *SLC12A3* gene. Electrophoresis of cDNA after PCR. *A*, Normal control leukocytes. *B*, Normal control kidney. *C*, Normal control urinary sediments. *D*, Patient's leukocytes. *E*, Patient's urinary sediments. *F*, The mother's leukocytes. For PCR, the forward primer located in exon 13 and the reverse primer located in exon 15 was used. Control samples clearly show a single band, whereas the samples extracted from leukocytes of the patient and the mother and urinary sediments of the patient show two bands, one the same size as the control sample and the other a larger one containing the cryptic exon sequence.

GAAGGTTGAGACTGACTGAGCCTTGGTGGCCTGTCTGGGGTCCCCCACCCTGGGAAGGAGGG
TGCCAAGCCAGTCCTTGGCAGAGTTGCCCAACAGGCTGTCCTCTCTCTCCCTGGGTCCCCGAAG
CTGAGCTCAACACCATAGCCCCCATCATTTCCAACTTCTTCCTCTGCTCCTATGCCCTCATCAACT Exon13 (102bp)
TCAGCTGCTTCCACGCCTCCATCACCAACTCGCCTGGTAAGCAAA------//------
GATGGTCTCGATCTCCTGACCTCATGATCCGCCCGCCTCAGCCTCCCAAAGTGCTGGGATTACA Intron13A (1076bp)
GTTGTGCCTGGCTGAGGAAGACTTTTTCTAACCAGCTCCAAATTGCCATTGTCTTTTACTAGGCC
ACCTTTTACATAGATCCCAATGTGTATGATGGCCCTGGAGTTGCACCATGAGGCAGCTGTCACT
AGTGGCAGCCCTGGCCTGACCTGCTGGTGGGGAGCCAGGCAGAATCATGTCCTTCCCCCTCCA Cryptic Exon (283bp)
TCTCACCCCCTTGGCACCATGGGAGCTGGTGCTGTTGCTGACATGGGATGTCCTGTGGCTGTAT
TTGGCCAGAGCTGGATGCTCCTGGTGAAATGCCAGCCAAAGCAGGCGTGTGATTTGCCCCAGA
GCCTGTAGACCCAGCCCAGGAGGCAGGGTGGGTGGTGCTCATGGCTGGTGGGTACAGGCTGG Intron13B (192bp)
GACCCCGGCTCTGGGCACTGCTGGCATTACTGCCAGGCCCTGCCCAGCAGCTCTGGCCTAGAA
AGAGGCTCGACTGCCAGGCATGCCCACTGACTGGTGCCCTTGGCCCAGGGTGGAGACCTTCAT
TCCAATACTACAACAAGTGGGCGGCGCTGTTTGGGGCTATCATCTCCGTGGTCATCATGTTCCT Exon14 (156bp)
CCTCACCTGGTGGGCGGCCCTCATCGCCATTGGCGTGGTGCTCTTCCTCCTGCTCTATGTCATCT
ACAAGAAGCCAGGTGCGCATCTCAGCTGCGGGGCCTCGGCCCTCCTCCCCCAGGGTAGCCATG
CAGGCGGCCCTGCCCTCCGCCCCAGTTGGAGGGCCCTGAGTCCGGCTCTGTGCT

Figure 3. Normal sequence surrounding intron 13. The cryptic exon sequence was derived from intron 13, which is positioned between AG and GC in normal genomic DNA.

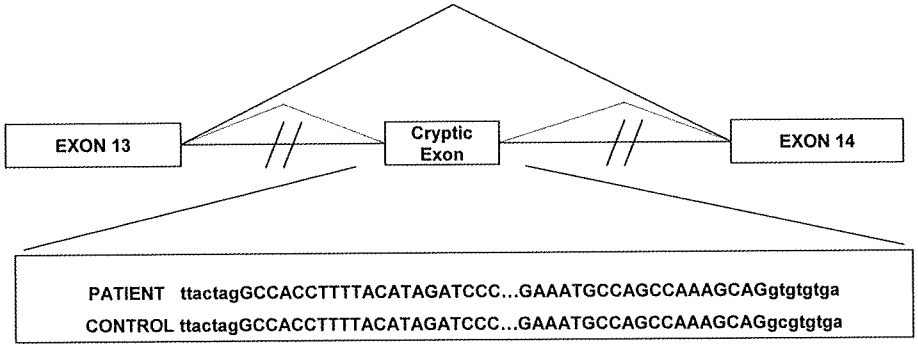

Figure 4. The schema of the intronic mutation resulting in the new splicing donor site for the cryptic exon.

create premature stop codons in exon 7 and in cryptic exon, respectively.

DISCUSSION

We identified two heterozygous mutations, c.818_819insG in the paternal allele and c.1670–191C>T in the maternal allele, in the genomic DNA from the leukocytes of a typical patient with GS, and we hypothesized that these compound heterozygous mutations of *SLC12A3* had caused GS in our patient. The latter mutation was confirmed to result in a splicing abnormality containing a cryptic exon in the transcripts. Amplification of *SLC12A3* mRNA extracted from the patient's leukocytes and urinary sediments, and the mother's leukocytes showed the same result for both extracts.

To date, >100 different mutations of the *SLC12A3* gene have been identified in the entire gene in patients with GS. These mutations are located all through the coding sequence of the *SLC12A3* gene, but most of them are found in the intracellular domains of the protein and missense mutations are the most frequently reported abnormalities. In previous studies, only one mutant allele was detected in 20 to 41% of patients with GS (3–7). There are many possible explanations for the nonidentification of the mutation in the second allele, for example, human error, direct sequencing missing major heterozygous mutations including rearrangements such as duplications, inversions, *etc.*, and the possible presence of mutations in gene-regulating fragments such as promoter or enhancer segments. It has also been hypothesized that there may be a concurrent heterozygous mutation in a gene other than the *SLC12A3* gene, particularly in the *CLCNKB* gene for type III Bartter syndrome (6). However, the exact reason for the nonidentification has not been established.

Because neither MLPA that was a recently established technique for detection of copy number variations nor *CLCNKB* gene analysis for detection of the modifier gene existence succeeded, we conducted RT-PCR analysis for detection of the deep intronic mutations, which were previously identified in other genes (11–13). As expected, we succeeded in detecting a deep intronic mutation that creates a new donor splice site resulting in the inclusion of a novel cryptic exon in mRNA. This molecular mechanism of intronic mutation may partly explain the poor success rate for detection of mutations in both alleles in patients with GS and demonstrates that single-base changes deep within introns can cause GS. Although, in GS, an intronic single-base substitution that leads to create cryptic splicing site has been reported, this patient showed intron 3 splicing acceptor consensus site mutation and resulted in the activation of a nearby cryptic splice site in intron 3 (14). This mutation can be easily detected by the analysis of exon-intron boundaries and our patient possessed a deep intronic mutation that is impossible to detect by genomic DNA analysis for detecting mutations in exons or exon-intron boundaries.

Igarashi *et al.* (15) were the first to identify transcript abnormalities by extracting mRNA from urinary sediment cells of patients with Dent disease. This method proved to be very useful for analyzing mRNA expression in renal tubular or glomerular cells in various kidney diseases. Renal biopsy

specimens constitute one source of material for analyzing mRNA in inherited kidney diseases, but renal biopsy is invasive and not needed for certain kidney diseases. Urinary sediments, on the other hand, contain cells derived from the kidney, and genetic analysis using those cells constitutes an entirely noninvasive, simple method for the diagnosis of inherited kidney diseases (10,16,17). Therefore, we conducted RT-PCR using urinary sediment cells to determine the presence of transcript abnormalities in the target organ cells.

This patient showed relatively severe symptoms including short stature, paralysis, muscle stiffness, and pain from her younger age. Recent report clearly showed that patients with GS and truncated mutations including out of frame splicing variants in at least one allele tend to show severe symptoms (18). Our patient also possessed truncated mutations caused by one base insertion and deep intronic mutation. These mutations may explain her severe symptoms.

To summarize, we investigated transcript abnormalities in a patient with GS caused by deep intronic mutation. This is the first report of GS associated with creation of a splice acceptor site by a deep intronic single-nucleotide change leading to the inclusion of extra exon structures, and this mutation could only have been detected *via* mRNA analysis. We identified a novel intronic mutation that may partly explain the poor success rate of mutation detection in both alleles in patients with GS and demonstrated that single-base changes deep within introns can cause GS.

REFERENCES

1. Gitelman HJ, Graham JB, Welt LG 1966 A new familial disorder characterized by hypokalemia and hypomagnesemia. Trans Assoc Am Physicians 79:221–235
2. Cruz DN, Shaer AJ, Bia MJ, Lifton RP, Simon DB 2001 Gitelman's syndrome revisited: an evaluation of symptoms and health-related quality of life. Kidney Int 59:710–717
3. Simon DB, Nelson-Williams C, Bia MJ, Ellison D, Karet FE, Molina AM, Vaara I, Iwata F, Cushner HM, Koolen M, Gainza FJ, Gitleman HJ, Lifton RP 1996 Gitelman's variant of Bartter's syndrome, inherited hypokalemic alkalosis, is caused by mutations in the thiazide-sensitive NaCl cotransporter. Nat Genet 12:24–30
4. Colussi G, Bettinelli A, Tedeschi S, De Ferrari ME, Syren ML, Borsa N, Mattiello C, Casari G, Bianchetti MG 2007 A thiazide test for the diagnosis of renal tubular hypokalemic disorders. Clin J Am Soc Nephrol 2:454–460
5. Lemmink HH, Knoers NV, Karolyi L, van Dijk H, Niaudet P, Antignac C, Guay-Woodford LM, Goodyer PR, Carel JC, Hermes A, Seyberth HW, Monnens LA, van den Heuvel LP 1998 Novel mutations in the thiazide-sensitive NaCl cotransporter gene in patients with Gitelman syndrome with predominant localization to the C-terminal domain. Kidney Int 54:720–730
6. Lin SH, Shiang JC, Huang CC, Yang SS, Hsu YJ, Cheng CJ 2005 Phenotype and genotype analysis in Chinese patients with Gitelman's syndrome. J Clin Endocrinol Metab 90:2500–2507
7. Monkawa T, Kurihara I, Kobayashi K, Hayashi M, Saruta T 2000 Novel mutations in thiazide-sensitive Na-Cl cotransporter gene of patients with Gitelman's syndrome. J Am Soc Nephrol 11:65–70
8. Fukuyama S, Okudaira S, Yamazato S, Yamazato M, Ohta T 2003 Analysis of renal tubular electrolyte transporter genes in seven patients with hypokalemic metabolic alkalosis. Kidney Int 64:808–816
9. Nozu K, Fu XJ, Nakanishi K, Yoshikawa N, Kaito H, Kanda K, Krol RP, Miyashita R, Kamitsuji H, Kanda S, Hayashi Y, Satomura K, Shimizu N, Iijima K, Matsuo M 2007 Molecular analysis of patients with type III Bartter syndrome: picking up large heterozygous deletions with semiquantitative PCR. Pediatr Res 62:364–369
10. Kaito H, Nozu K, Fu XJ, Kamioka I, Fujita T, Kanda K, Krol RP, Suminaga R, Ishida A, Iijima K, Matsuo M 2007 Detection of a transcript abnormality in mRNA of the SLC12A3 gene extracted from urinary sediment cells of a patient with Gitelman's syndrome. Pediatr Res 61:502–505
11. King K, Flinter FA, Nihalani V, Green PM 2002 Unusual deep intronic mutations in the COL4A5 gene cause X linked Alport syndrome. Hum Genet 111:548–554
12. Ogino W, Takeshima Y, Nishiyama A, Okizuka Y, Yagi M, Tsuneishi S, Saiki K, Kugo M, Matsuo M 2007 Mutation analysis of the ornithine transcarbamylase (OTC) gene in five Japanese OTC deficiency patients revealed two known and three novel mutations including a deep intronic mutation. Kobe J Med Sci 53:229–240
13. Yagi M, Takeshima Y, Wada H, Nakamura H, Matsuo M 2003 Two alternative exons can result from activation of the cryptic splice acceptor site deep within intron 2 of the dystrophin gene in a patient with as yet asymptomatic dystrophinopathy. Hum Genet 112:164–170
14. Abuladze N, Yanagawa N, Lee I, Jo OD, Newman D, Hwang J, Uyemura K, Pushkin A, Modlin RL, Kurtz I 1998 Peripheral blood mononuclear cells express mutated NCCT mRNA in Gitelman's syndrome: evidence for abnormal thiazide-sensitive NaCl cotransport. J Am Soc Nephrol 9:819–826
15. Igarashi T, Inatomi J, Ohara T, Kuwahara T, Shimadzu M, Thakker RV 2000 Clinical and genetic studies of CLCN5 mutations in Japanese families with Dent's disease. Kidney Int 58:520–527
16. Iida K, Nozu K, Takahashi Y, Okimura Y, Kaji H, Matsuo M, Chihara K 2008 Characterization of a splicing abnormality in Gitelman syndrome. Am J Kidney Dis 51:1077–1078
17. Krol RP, Nozu K, Nakanishi K, Iijima K, Takeshima Y, Fu XJ, Nozu Y, Kaito H, Kanda K, Matsuo M, Yoshikawa N 2008 Somatic mosaicism for a mutation of the COL4A5 gene is a cause of mild phenotype male Alport syndrome. Nephrol Dial Transplant 23:2525–2530
18. Riveira-Munoz E, Chang Q, Godefroid N, Hoenderop JG, Bindels RJ, Dahan K, Devuyst O 2007 Transcriptional and functional analyses of SLC12A3 mutations: new clues for the pathogenesis of Gitelman syndrome. J Am Soc Nephrol 18:1271–1283

Pediatr Nephrol (2009) 24:1181–1186
DOI 10.1007/s00467-009-1119-8

ORIGINAL ARTICLE

Minimal change nephrotic syndrome associated with immune dysregulation, polyendocrinopathy, enteropathy, X-linked syndrome

Yuya Hashimura · Kandai Nozu · Hirokazu Kanegane · Toshio Miyawaki · Akira Hayakawa · Norishige Yoshikawa · Koichi Nakanishi · Minoru Takemoto · Kazumoto Iijima · Masafumi Matsuo

Received: 3 November 2008 / Revised: 5 January 2009 / Accepted: 5 January 2009 / Published online: 3 February 2009

Abstract Several studies have suggested that T cell-producing permeability factors might lead to proteinuria in minimal change nephrotic syndrome (MCNS). However, it is still unclear whether T-cell abnormalities cause MCNS. Immune dysregulation, polyendocrinopathy, enteropathy, X-linked (IPEX) syndrome is a rare disorder of the immune regulation system, which leads to severe autoimmune phenomena including autoimmune enteropathy, atopic dermatitis with high levels of serum immunoglobulin E (IgE), type 1 diabetes mellitus (T1DM), and severe infection such as sepsis, which frequently result in death within the first 2 years of life. This disease is caused by mutations in the *FOXP3* gene that result in the defective development of regulatory T (Treg) cells. This report describes a 5-year-old boy with IPEX syndrome with a 3 bp deletion in the *FOXP3* gene (c.748–750delAAG, p.250K.del) and a paucity of $CD4^+$ $CD25^+$ $FOXP3^+$ T cells. The boy's condition was complicated by MCNS in addition to many IPEX-related manifestations, such as atopic dermatitis, T1DM, enteropathy, sepsis and hemolytic anemia. This is the first report of IPEX syndrome complicated by MCNS, and our findings imply that Treg cell dysfunction may be crucial for the development of MCNS.

Keywords Immune dysregulation, polyendocrinopathy, enteropathy, X-linked (IPEX) syndrome · Minimal change nephrotic syndrome · FOXP3 · Regulatory T cell

Y. Hashimura · K. Nozu · A. Hayakawa · M. Matsuo
Department of Pediatrics,
Kobe University Graduate School of Medicine,
Kobe, Japan

H. Kanegane · T. Miyawaki
Department of Pediatrics, Graduate School of Medicine,
University of Toyama,
Toyama, Japan

N. Yoshikawa · K. Nakanishi
Department of Pediatrics, Wakayama Medical University,
Wakayama, Japan

M. Takemoto
Clinical Cell Biology and Medicine, Graduate School
of Medicine, Chiba University,
Chiba, Japan

K. Iijima (✉)
Division of Child Health and Development,
Department of Pediatrics,
Kobe University Graduate School of Medicine,
5-1 Kusunoki-cho 7 chome, Chuo-ku,
Kobe 650-0017, Japan
e-mail: iijima@med.kobe-u.ac.jp

Introduction

In 1974 Shalhoub [1] proposed the hypothesis that "lipoid nephrosis", now known as minimal change nephrotic syndrome (MCNS), is a disorder of T cell function resulting in the production of a circulating lymphokine toxin (later termed a vascular permeability factor) because of limited humoral immunity and immune effectors in glomeruli, remission associated with measles infection or with corticosteroids and cyclophosphamide treatment, and simultaneous occurrence of Hodgkin's disease or thymoma. However, this interesting hypothesis has not yet been definitively validated.

Immune dysregulation, polyendocrinopathy, enteropathy, X-linked (IPEX) syndrome is a rare disorder of the immune

regulation system, which results in multiple autoimmune disorders and is characterized by X-linked recessive inheritance [2]. Children with IPEX syndrome develop severe autoimmune phenomena, including autoimmune enteropathy, atopic dermatitis with high levels of serum immunoglobulin E (IgE), type 1 diabetes mellitus (T1DM), and severe infection such as sepsis, which frequently result in death within the first 2 years of life. IPEX is caused by mutations in the *FOXP3* gene that result in the defective development of $CD4^+$ $CD25^+$ regulatory T (Treg) cells which constitute an important T cell subset involved in immune homeostasis and protection against autoimmunity [3]. The disease gene, *FOXP3*, was identified in 2001, and several mutations within this gene have been detected in patients with IPEX syndrome [4].

This report described a 5-year-old boy with IPEX syndrome associated with MCNS, as well as atopic dermatitis, T1DM, enteropathy, sepsis, hemolytic anemia and high serum IgE level. This is the first report of IPEX syndrome associated with MCNS.

Materials and methods

Case report

A 5-year old Japanese boy was in good health until 2 months of age, when he developed atopic dermatitis and milk allergy. At 4 months of age he presented with polyposia and polyuria, and he was diagnosed with T1DM. When he was 1 year old, he developed nephrotic syndrome, which was steroid-sensitive but also frequent-relapsing nephrotic syndrome. He was therefore treated with cyclosporine and remained in remission during treatment. He underwent renal biopsy 2 years after the start of the cyclosporine regimen, and light microscopy showed minor glomerular abnormalities without tubulointerstitial lesions including chronic cyclosporine nephrotoxicity (Fig. 1). Immunofluorescence microscopy showed all negative findings (IgG, IgA, IgM, C1q, C3, C4 and fibrin). Thus, he was diagnosed with MCNS without chronic cyclosporine nephrotoxicity. Cyclosporine treatment was therefore continued. When he was 5 years old he started vomiting after contracting varicella chicken pox, from which he recovered, but without regression in vomiting. When cyclosporine was discontinued, his vomiting soon worsened, and he developed recurrent sepsis caused by *Acinetobacter baumannii* and failure to thrive. At that time, he was referred to Kobe University Hospital.

On admission, his body mass index was only 12, indicating malnutrition. His hemoglobin level was 7.8 g/dl, and the result of a direct Coombs test was positive, suggesting autoimmune hemolytic anemia. His renal function was normal, but the IgE level was very high (1,141 IU/ml). He had hyperglycemia (glucose 373 mg/dl), but normal thyroid function. Treatment with multiple antibiotics resulted in gradual recovery from sepsis. However, he still was suffering from vomiting and failure to thrive. Although his mother, father and sisters were healthy, his mother's two brothers had died at the age of 1 year due to sepsis. On the basis of his symptoms and family history, we suspected that he was suffering from IPEX syndrome. We therefore carried out genetic and flow cytometric analysis of FOXP3 and started therapy with high doses of methylprednisolone and cyclosporine. Soon afterwards, his appetite recovered and the vomiting disappeared. He underwent repeat renal biopsy, and he was diagnosed with MCNS again.

Informed consent for genetic and flow cytometric analysis of FOXP3 was obtained from the patient's parents.

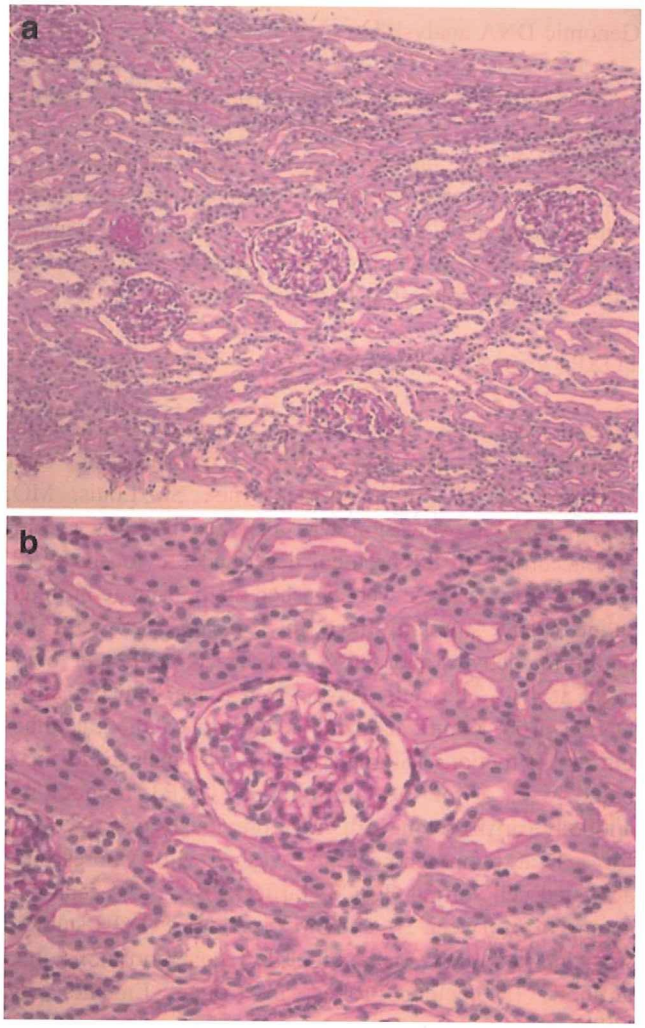

Fig. 1 Renal biopsy findings. **a** Periodic acid–Schiff (PAS) staining ×200; **b** PAS staining ×400. The renal biopsy specimen obtained 2 years after cyclosporine treatment showed minor glomerular abnormalities without tubulointerstitial lesions, including chronic cyclosporine nephrotoxicity